Charged Component of 1-GeV Electron Showers in Lead*

D. J. DRICKEY

Stanford Linear Accelerator Center, Stanford University, Stanford, California

AND

J. R. KILNER

Philco-Ford Corporation, Space and Re-entry Systems Division, Palo Alto, California

AND

D. BENAKSAS

Laboratoire de l'Accelerateur Lineaire, Orsay, France

(Received 5 February 1968)

Electron showers from 1-GeV electrons incident on 1–10 radiation lengths of lead have been observed in a streamer chamber placed in a magnetic field. The experimental technique was essentially 100% efficient in delineating showers containing either zero or many charged shower particles, permitting a significant increase in accuracy over previous experimental results on shower development. Results are presented for the number of shower electrons present having energies above 5-, 10-, and 25-MeV cutoffs. The data presented have typical errors of about 6% and show good agreement with the results of recent Monte Carlo calculations.

INTRODUCTION

ELECTRON showers produced by incident electrons or photons are an excellent example of that class of electrodynamic processes that are in principle completely understood analytically but in practice require involved Monte Carlo programs in order to calculate them adequately. These programs represent a theory of the process that must be experimentally checked, at least in some aspects, if the entire predicted distributions are to be regarded as valid. A disagreement between theory and experiment in such a case probably does not represent a breakdown of the fundamental physical principles involved in the problem, but rather would represent neglect of some physical process or a mistake in the program. In any case, the proof of the validity of these calculations must be based on experimental results.

Historically, the first Monte Carlo calculations on shower development were done by Wilson.[1] These results were later corrected and provide an excellent fit to experimental data within the statistical limits.[2] More elaborate calculations have been performed by Messel et al.[3] We have compared our experiments with the recent calculations of Nagel,[4] which have been extended to 6 GeV by Völkel.[5] They have improved the previous Monte Carlo shower calculations by extending them to lower cutoff energies.

Experimental checks of these calculations have been performed by a variety of methods. These experiments divide into two principal classes, those that measure the total energy deposition at various points in the shower and those that concentrate on measuring the number and energy of electrons in the shower. The first class measures the energy loss due to the electron component of all energies, traveling in all directions. One example is the pioneering experiment of Hofstadter and Kantz,[6] who used sodium-iodide crystals viewed by phototubes to measure shower characteristics. This method has also been used recently in a thorough study of shower energy deposition by Crannell.[7] Energy deposition has also been studied by Nelson et al.,[8] who used thermoluminescent dosimetry techniques (TLD) in lithium-fluoride crystals and concentrated primarily on measuring the radial development of showers. Ionization chambers[9] have been used to probe the energy deposition as has photographic film[10] and nuclear emulsions.[11]

The second experimental technique concentrates on observation of the charged component of the shower by counting tracks produced by electrons or positrons present at different depths in the shower. This component has been observed by spark chambers,[12] lead-plastic "sandwich" counters,[13] and cloud chambers lacking a magnetic field.[14] These experiments suffer from the fact that the cutoff energy, i.e., the lowest-

---

* Work supported in part by the U.S. Office of Naval Research under Contract No. Nonr 225(67).

[1] R. R. Wilson, Phys. Rev. **86**, 261 (1952).

[2] H. Thom, Phys. Rev. **136**, B447 (1964).

[3] H. Messel, A. D. Smirnov, A. A. Varfolomev, D. F. Crawford, and J. C. Butcher, Nucl. Phys. **39**, 1 (1962); D. F. Crawford and H. Messel, Phys. Rev. **128**, 2352 (1962); Nucl. Phys. **61**, 145 (1965).

[4] H. H. Nagel, Z. Physik **186**, 319 (1965).

[5] U. Völkel, Deutsches Elektronen-Synchrotron Report No. DESY 6516 (unpublished).

[6] A. Kantz and R. Hofstadter, Phys. Rev. **89**, 607 (1953).

[7] C. J. Crannell, Phys. Rev. **161**, 310 (1967).

[8] W. R. Nelson, T. M. Jenkin, R. C. McCall, and J. K. Cobb, Phys. Rev. **149**, 201 (1966).

[9] W. Blocker, R. W. Kenney, and W. K. H. Panofsky, Phys. Rev. **89**, 607 (1953).

[10] Y. Murata, J. Phys. Soc. Japan **20**, 209 (1965).

[11] M. Akashi, K. Shimizu, Z. Watanabe, T. Ogawa, N. Ogita, A. Misaki, I. Mito, S. Oyama, S. Tokurega, M. Fujimoto, S. Hasegawa, J. Nishimura, K. Niu, and K. Yoki, J. Phys. Soc. Japan **17**, Suppl. A-III, Part III, 427 (1962).

[12] J. W. Cronin, E. Engels, M. Pyka, and R. Roth, Rev. Sci. Instr. **33**, 946 (1962).

[13] C. A. Heusch and C. Y. Prescott, Phys. Rev. **135**, B772 (1964).

[14] E. Becklin and J. Earl, Phys. Rev. **136**, B237 (1964).

energy particle observable in the experiment, is only approximately known.

Experiments most closely related to the present one are those that use a magnetic field to define this cutoff and permit, at least in principle, a direct comparison with the calculations for various values of the cutoff energy. Such experiments have been performed in cloud chambers with magnetic field[15] and bubble chambers.[16] We have chosen to use a new technique, a streamer chamber[17] placed in a magnetic field, to observe the number and energies of electrons emerging from lead at various depths in a shower produced by 1-GeV electrons. This instrument seems ideally suited to such an experiment since it supports many tracks (several hundred have been seen in a single photograph), permits a measurement of the recoil momenta, and may be triggered on an event.

EXPERIMENTAL SETUP

Figure 1 shows the experimental arrangement at the Mark III linear accelerator at Stanford for this experiment. The experiment was performed in the low-intensity parasitic beam at that accelerator.[18]

The incident photons come from the collimator located at the end of the accelerator and are a byproduct of other experiments using the primary beam in a research area upstream from the one shown in Fig. 1. These photons produce pairs in a converter, the resultant positrons or electrons being energy analyzed in the three-magnet analysis system of the "south switch-yard." Beam size is limited by a collimator in the wall between the switchyard and experimental area. In the present experiment the parasitic beam was used at about one positron per second and at an energy of 1 GeV, with a momentum resolution of less than $\Delta p/p = 5\%$.

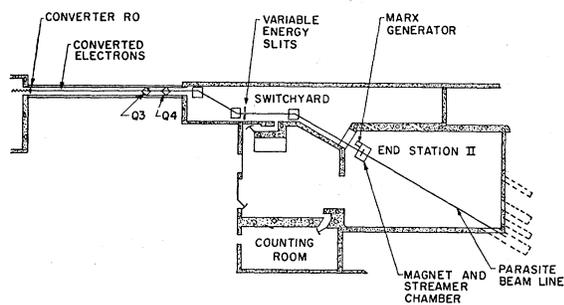Positrons were incident on the streamer chamber arrangement shown in Fig. 2. The driving system con-

Fig. 1. Layout of the experimental area showing the parasite beam and the streamer chamber and magnet arrangement.

[15] M. D. Wilson and I. B. McDiarmid, Can. J. Phys. **40**, 573 (1962).
[16] H. Lengeler, W. Tejessy, and M. Deutschmann, Z. Physik **175**, 283 (1963).
[17] F. Bulos, A. Odian, F. Villa, and D. Yount, Stanford Linear Accelerator Report No. 74, 1967 (unpublished).
[18] D. J. Drickey, Stanford University High Energy Physics Laboratory Report No. HEPL-542, 1967 (unpublished).
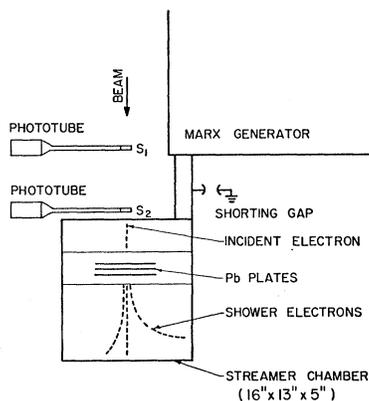
Fig. 2. Streamer chamber arrangement for this experiment.

sisted of a Marx generator developing about 250 kV that drove the streamer chamber essentially as a capacitor. The high-voltage pulse was "chopped" by a shorting gap timed to fire shortly after the Marx fired. Resistor chains located at three of the four corners of the streamer chamber were empirically adjusted to aid in forming the $\simeq$10 nsec, 200-kV pulse necessary for proper operation of the 12-cm gap chamber.

The streamer chamber, 30 cm long in the beam direction, was divided into three sections with lengths of 11, 13, and 15 cm, respectively, as shown in Fig. 2. The first section (upbeam, 11 cm long) was used to ensure the fact that one and only one electron was incident on the lead plates, and also provided direct evidence that the chamber had fired properly. This latter point was extremely important in ensuring valid results. The alternative method—of merely placing lead plates outside of and upbeam from a single streamer chamber—creates confusion between those cases when no charged particle emerges from the lead and when the chamber fires improperly. Lead plates were inserted in the second (middle, 13-cm-long) section of the chamber where the high-voltage plate had been cut away to prevent breakdown to the lead plates. The downbeam surface of the lead converter was 4.5 cm upbeam from the entrance to the third section of the chamber (15 cm long) in which shower particles were observed and measured. Data were taken with lead converters of thickness 1, 2, 3, 4, 5, 6, 8, and $10X_0$ ($X_0 = 0.51$ cm).

Photography was performed using two 35-mm cameras directly in narrow angle stereo; each camera also viewed two mirrors providing 90° stereo and a back view. Kodak 2475 film was used in one camera, Kodak SO340 in the other. About 4000 pictures were taken providing typically about 150 useable events at each radiator thickness. The 12-cm gap of the chamber necessitated a geometric correction to the data since the chamber did not subtend the complete 2π sr. A magnetic field of 1665 G$\pm$~1% was chosen as the most convenient value providing reasonable momentum resolution without undue distortion of the low-energy shower components.

TABLE I. Mean number of electrons with energy greater than 10 MeV from 1-GeV electron showers in lead. At each radiator thickness, the geometrical acceptance correction, the corrected mean number of electrons from Monte Carlo calculations, and the experimentally measured mean number of electrons are given.

X_0	Acceptance correction	Corrected theoretical mean	Experimental mean
1	0.97	2.20	2.28±0.13
2	0.92	3.54	3.69±0.13
3	0.88	4.06	3.61±0.16
4	0.86	3.65	3.66±0.15
5	0.85	2.93	2.89±0.20
6	0.84	2.11	1.84±0.13
8	0.82	1.12	1.29±0.09
10	0.83	0.56	0.46±0.07

DATA ANALYSIS

The primary criterion for the selection of an event (such as that shown in Fig. 2) for analysis was the presence of a single track in the first section of the streamer chamber. Acceptable tracks in the third section were also required to be neither too dark nor too light and to penetrate at least 1 in. into the third section. The selected events were projected in a simple film reader and the curvatures of the secondary tracks were compared with curves on a template drawn with curvatures corresponding to electrons with cutoff energies of 5, 10, and 25 MeV and with energies of 10% above and below these values. The magnetic field within the streamer chamber was chosen to optimize the accuracy of measuring the curvature of 10-MeV electron tracks. The templates were used to determine only which of the cutoff energies were exceeded by an electron, rather than to determine the energy of the electron itself. This simplified the scanning, especially when the electron energy did not lie near one of the three chosen cutoff values. In general, it was possible to determine the better fitting of two template curves differing by 10% in curvature. A correction was made for the effect on the energy of the angle between the particle track and the plane normal to the magnetic field (the dip angle). Measurements were made primarily in one of the top (horizontal plane) views, the other views serving as a check and allowing a determination of the dip angles. All the events were scanned twice.

The acceptance solid angle of the streamer chamber is significantly less than the forward hemisphere over which the calculations of Nagel[4] were performed. Consequently, it is necessary to make corrections either to the experimental data or to the theoretical calculations, before the two may be compared. We have chosen to plot the experimental data without modification and to make all the corrections to the Monte Carlo results, using only the geometry of the streamer chamber and the tabulations of Nagel in calculating these corrections. Even though secondary electrons emitted from the converter at large angles to the shower axis

miss the streamer chamber, the magnitude of the corresponding corrections remains reasonably small because the shower electrons are strongly peaked in the forward direction. An outline of the method used in computing the acceptance correction follows.

The fraction $A(\theta, E)$ of secondary electrons emerging from the target with an energy E and an angle θ (with respect to the beam direction or shower axis) penetrating at least 1 in. into the third section of the streamer chamber was calculated from the geometrical relations of the target and the streamer chamber, taking into account the curvature of the electrons in the magnetic field. An approximation to the angular distribution $B(\theta, E, X)$ for the secondary electrons emerging from a target of thickness X with energy E was reconstructed from the data contained in Nagel's tables for the angular distributions at various cutoff energies. Although only an approximate angular distribution could be so obtained, only a small error results since the correction was moderately insensitive to the shape of $B(\theta, E, X)$. The geometrical acceptance $A(\theta, E)$ weighted by the
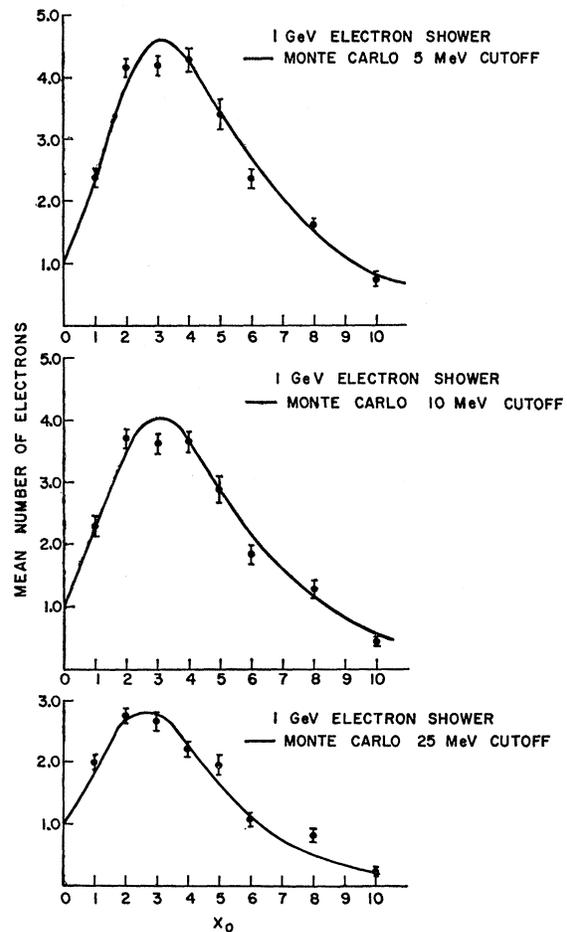

FIG. 3. Average shower curves from 1-GeV electrons incident on lead. Top, 5-MeV cutoff; middle, 10-MeV cutoff; and bottom, 25-MeV cutoff.

TABLE II. $P(N)$, the probability of seeing N electrons above 10 MeV at a given radiation length and from a 1-GeV electron shower in lead. The corrected Monte Carlo results are presented above the corresponding experimentally observed value with error.

X_0	0	1	2	3	4	5	6	7	8	9	10
1	0.019	0.448	0.150	0.220	0.083	0.049	0.023	0.006	0.003	0.001	0.000
	0.021	0.387	0.169	0.232	0.127	0.028	0.035	0.000	0.000		
	±0.012	±0.041	±0.031	±0.035	±0.028	±0.014	±0.016	±0.007	±0.007		
2	0.025	0.125	0.179	0.221	0.169	0.123	0.068	0.046	0.025	0.011	0.004
	0.018	0.103	0.178	0.214	0.165	0.143	0.094	0.058	0.009	0.009	0.009
	±0.009	±0.019	±0.026	±0.027	±0.025	±0.023	±0.019	±0.013	±0.006	±0.006	±0.006
3	0.022	0.080	0.130	0.181	0.189	0.168	0.103	0.068	0.034	0.015	0.006
	0.021	0.062	0.186	0.262	0.172	0.165	0.076	0.041	0.007	0.000	0.007
	±0.012	±0.020	±0.032	±0.037	±0.031	±0.031	±0.022	±0.017	±0.007	±0.007	±0.007
4	0.034	0.098	0.173	0.193	0.189	0.146	0.086	0.043	0.023	0.010	0.004
	0.036	0.060	0.199	0.217	0.205	0.114	0.090	0.036	0.012	0.030	0.000
	±0.015	±0.019	±0.031	±0.032	±0.032	±0.025	±0.022	±0.015	±0.009	±0.013	±0.006
5	0.069	0.157	0.208	0.227	0.158	0.099	0.049	0.024	0.008	0.002	0.000
	0.053	0.171	0.250	0.237	0.132	0.053	0.053	0.026	0.013	0.013	0.000
	±0.026	±0.043	±0.050	±0.049	±0.039	±0.026	±0.026	±0.019	±0.013	±0.013	±0.013
6	0.154	0.263	0.233	0.162	0.104	0.054	0.023	0.007	0.002	0.001	0.000
	0.243	0.224	0.252	0.112	0.103	0.037	0.019	0.009	0.000	0.000	
	±0.041	±0.040	±0.042	±0.031	±0.029	±0.019	±0.013	±0.009	±0.009	±0.009	
8	0.388	0.300	0.183	0.089	0.027	0.009	0.003	0.001	0.001	0.000	0.000
	0.364	0.292	0.185	0.079	0.033	0.026	0.013	0.007	0.000		
	±0.039	±0.037	±0.032	±0.022	±0.015	±0.013	±0.009	±0.007	±0.007		
10	0.635	0.234	0.089	0.029	0.010	0.003	0.001	0.000	0.000	0.000	0.000
	0.666	0.238	0.060	0.036	0.000	0.000	0.000				
	±0.051	±0.047	±0.026	±0.020	±0.012	±0.012	±0.012				

angular distribution $B(\theta, E, X)$ gives

$$C(\theta, E_0, X)$$

$$= \int_{E_0}^{E_{max}} A(\theta, E) B(\theta, E, X) dE \Big/ \int_{E_0}^{E_{max}} B(\theta, E, X) dE,$$

where E_0 is the cutoff energy. This was folded into the angular distributions $D(\theta, E_0, X)$ given by Nagel to obtain the acceptance correction $F(E_0, X)$;

$$F(E_0, X) = \int_0^{\pi/2} D(\theta, E_0, X) C(\theta, E_0, X) d\theta.$$

F (10 MeV, X) is given in Table I in the column labeled "acceptance correction." The acceptance correction $F(E_0, X)$ was also calculated from the preceding equation by replacing $C(\theta, E_0, X)$ by $A(\theta, E_0)$, thus neglecting the variation in the angular distribution with energy. The difference between the two calculations was always less than 3%.

To simplify the calculation of the acceptance correction, it was assumed that all shower particles emerged from the center of the downbeam face of the converter, or at a point on the shower axis. The error resulting from this assumption was checked by repeating a typical calculation with the point of emergence of the secondary electrons shifted by 0.5 in. (the beam half-width) either vertically or horizontally. The magnitude of the correction changed by less than 1% in both cases.

Nagel tabulates the probability $P_0(N, E_0, X)$ of observing exactly N secondary electrons in the forward hemisphere above an energy E_0 from a converter of thickness X radiation lengths. Since the solid angle of the streamer chamber is less than the 2π sr for which Nagel's calculations apply, we modify his calculated $P_0(N, E_0, X)$ to correspond to the geometry used in this experiment. To do this, it is necessary to make the assumption that the angular distribution of the secondary electrons is independent of N. Then the probability of any electron's entering the acceptance region of the chamber is the same and its value is given by the acceptance correction discussed above. Applying this correction to $P_0(N, E_0, X)$, we obtain the probability $P(N, E_0, X)$ of observing N electrons within the streamer chamber above an energy E_0 from a target of thickness X. This probability is tabulated in Table II for $E_0 = 10$ MeV and is shown in the curves of Fig. 4 for 5, 10, and 25 MeV.

ERRORS

In addition to the statistical errors due to the random counting process, a number of other sources of error in the comparison between the experimental data and corrected theoretical results are present. Although some
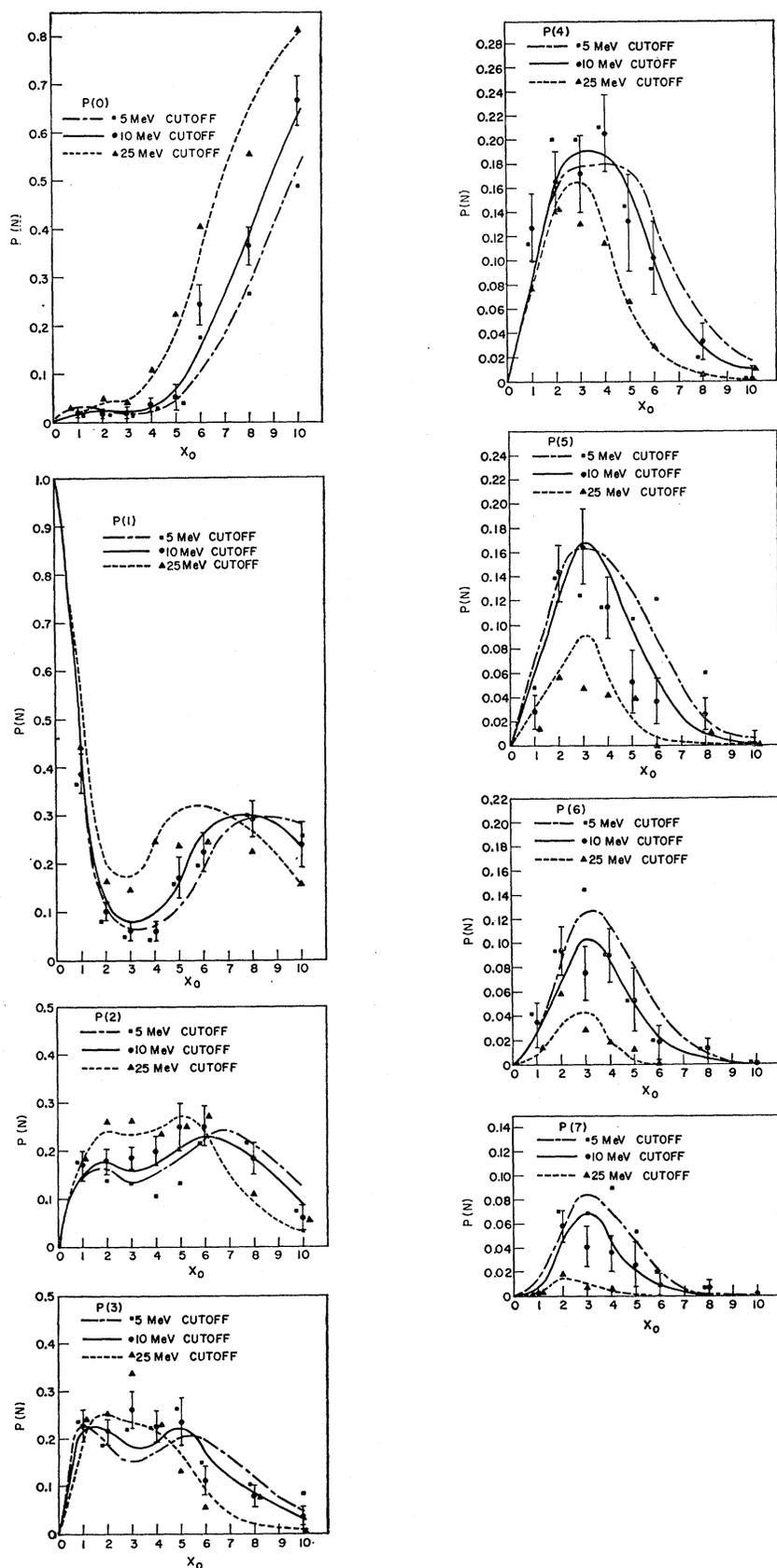
Fig. 4. Probability distributions for 1-GeV showers in lead. $P(N)$ is the probability of seeing N electrons or positrons above a given cutoff energy at a depth X_0 radiation lengths. Error bars have been suppressed for clarity on the 5- and 25-MeV cutoff data but are comparable to those shown on the 10-MeV data. Notice the scale change at $P(4)$.

of these can be determined only approximately, it is believed that they all have a magnitude of generally less than 2%.

The errors due to the experimental parameters are as follows:

(1) The magnetic field is known (and is uniform) to within 2%.

(2) The measurements of the dimensions and positions of the apparatus components are good to within 2%.

(3) The primary electron central energy is 1.00 GeV±2%, with a width of less than 6%, and produces a much smaller effect on the data since the distributions measured are fairly insensitive to it.

The errors produced in the scanning process are as follows:

(1) The cutoff energy E_0 is measured to approximately 8% accuracy. This results in an error in the measured distributions of typically 1% and at most 3%. This includes the error in the templates used for this measurement and the error in measuring the dip angles (which is approximately 5%).

(2) Masked or uncounted tracks probably occur less than 2% of the time.

The errors in the acceptance correction calculation are as follows:

(1) The graphical methods used have an accuracy of approximately 2%.

(2) The beam position and finite beam size produce an error of less than 1%, as discussed above.

These errors may be combined to obtain an approximate error of 5% excluding the counting statistical error. This is consistent with the good agreement of data with the corrected calculations of Nagel.

RESULTS

Tables I and II summarize our experimental results for 1-GeV electron showers in lead. We list here the data with a 10-MeV cutoff but include the 5- and 25-MeV cutoff data in all curves. In this sense, the 5- and 25-MeV data are considered only as experimental checks that no significant energy bias exists in the data. In Table I we list the fractional correction to Nagel's Monte Carlo data, the corrected theoretical mean number of electrons, and the experimental mean number of electrons with error. Excellent agreement exists between the experimental data and the Monte

Carlo results within the experimental error of approximately 6%.

Table II gives the distribution $P(N)$, the probability that N particles are seen at a given depth in a shower. Nagel's results as modified to our geometry are presented along with our experimental result and error. Our results and the calculations are in good agreement.

Figure 3 shows the experimental results for the mean number of electrons at the three cutoff energies, 5, 10, and 25 MeV. The solid curves are Nagel's results corrected to our geometry, and the resultant fits are good. No systematic bias in the data is apparent in the comparison of the three cutoff energies, with the possible exception of the point at $3X_0$, where the data appear systematically low. We ascribe this to a statistical effect.

In Fig. 4 we present the probability distributions $P(N)$ for $N = 1-7$. The Monte Carlo results for 5-, 10-, and 25-MeV cutoff energies are shown as curves. Experimental points with errors are shown for the 10-MeV cutoff energy points. The experimental points for 5- and 25-MeV cutoff energies have comparable errors and the error bars have been suppressed for clarity. Good agreement with the theoretical curves is seen. The excellent fit to $P(0)$ is especially important since this demonstrates that experimental inefficiencies were small and that we were able to identify successfully the cases when only photons were present in the shower.

CONCLUSIONS

Monte Carlo calculations for 1-GeV electron showers in lead have been checked to a statistical precision of about 6% and an over-all precision of about 8%. Excellent agreement between the experiment and the calculation is found. The experimental technique permits good definition of the cutoff energy and the sensitivity of the experiment to the value of the cutoff energy is found to be large. The accurate cutoff energy definition and the accuracy of identifying the case when no charged particle is present in the shower represent significant improvements in technique over previous experiments.

ACKNOWLEDGMENTS